Estuaries Vol. 24, No. 5, p. 655–669 October 2001

Reconsidering the Physics of the Chesapeake Bay Estuarine Turbidity Maximum

LAWRENCE P. SANFORD[1,*], STEVEN E. SUTTLES[1], and JEFFREY P. HALKA[2]

[1] *University of Maryland Center for Environmental Science, Horn Point Laboratory, P. O. Box 775, Cambridge, Maryland 21613*

[2] *Maryland Geological Survey, 2300 St. Paul Street, Baltimore, Maryland 21218*

ABSTRACT: A series of cruises was carried out in the estuarine turbidity maximum (ETM) region of Chesapeake Bay in 1996 to examine physical and biological variability and dynamics. A large flood event in late January shifted the salinity structure of the upper Bay towards that of a salt wedge, but most of the massive sediment load delivered by the Susquehanna River appeared to bypass the ETM zone. In contrast, suspended sediments delivered during a flood event in late October were trapped very efficiently in the ETM. The difference in sediment trapping appeared to be due to increases in particle settling speed from January to October, suggesting that the fate of sediments delivered during large events may depend on the season in which they occur. The ETM roughly tracked the limit of salt (defined as the intersection of the 1 psu isohaline with the bottom) throughout the year, but it was often separated significantly from the limit of salt with the direction of separation unrelated to the phase of the tide. This was due to a lag of ETM sediment resuspension and transport behind rapid meteorologically induced or river flow induced motion of the salt limit. Examination of detailed time series of salt, suspended sediment, and velocity collected near the limit of salt, combined with other indications, led to the conclusion that the convergence of the estuarine circulation at the limit of salt is not the primary mechanism of particle trapping in the Chesapeake Bay ETM. This convergence and its associated salinity structure contribute to strong tidal asymmetries in sediment resuspension and transport that collect and maintain a resuspendable pool of rapidly settling particles near the salt limit. Without tidal resuspension and transport, the ETM would either not exist or be greatly weakened. In spite of this repeated resuspension, sedimentation is the ultimate fate of most terrigenous material delivered to the Chesapeake Bay ETM. Sedimentation rates in the ETM channel are at least an order of magnitude greater than on the adjacent shoals, probably due to focusing mechanisms that are poorly understood.

Introduction

The estuarine turbidity maximum (ETM) zone of upper Chesapeake Bay, a region of elevated suspended sediment concentrations and reduced light availability near the limit of salt intrusion, was first studied in the late 1960s and early 1970s. The most extensive work was carried out by Schubel (1968a,b, 1971), Schubel and Biggs (1969), and Schubel and Kana (1972), who mapped the spatial and seasonal variability of the ETM, examined tidal resuspension processes at its center, and carried out studies of suspended particles and agglomerates. Biggs (1970) also considered the sediment budget of the upper Bay, while Nichols (1974, 1977) examined the dynamics of the ETM in the Rappahannock, a southern tributary of the Chesapeake Bay.

These early studies provided good descriptions of ETMs in the partially mixed Chesapeake Bay and its tributaries, but they were limited in their ability to address dynamical questions for several reasons. First, they were technology limited; Schubel (1968a) obtained a large data set on the distribution of suspended sediment in and near the Chesapeake ETM, but he reported just a few observations of currents, no salinity data, and no settling velocity data. Second, there were few other reported ETM studies for comparison, and there was a limited understanding of the dynamical complexities of ETM particle trapping. While Schubel (1968b) recognized the importance of tidal resuspension for maintaining high suspended sediment concentrations, he and other researchers (Festa and Hansen 1978; Officer 1980) attributed ETM particle trapping primarily to the convergence of the estuarine circulation at the limit of salt intrusion combined with slow particle settling.

In the years since these initial studies of the Chesapeake Bay ETM, other investigators have shown that mechanisms of particle trapping in ETMs are more complex than simple convergence of the estuarine circulation. Dyer (1988) and Dyer and Evans (1989) showed how a phase lag of sediment resuspension relative to near-bottom currents can produce an ETM in the presence of

* Corresponding author; tele: 410/228-8200; fax: 410/221-8490; e-mail: lsanford@hpl.umces.edu.

asymmetrical tidal currents without convergence of the gravitational circulation. Geyer (1993) showed that suppression of turbulent mixing by density stratification downstream of the limit of salt intrusion amplified trapping efficiency for a range of particle settling velocities faster than those proposed by Festa and Hansen (1978). Hamblin (1989) demonstrated that a combination of ebb-flood asymmetry in suspended sediment transport and suppression of mixing by density stratification were likely responsible for particle trapping in the St. Lawrence ETM. Jay and Musiak (1994) reported that strong tidal asymmetries in stratification and flow near the salt limit likely explain suspended-sediment trapping in the Columbia River ETM. Uncles and Stephens (1993) demonstrated that the location of a pool of resuspendable particles defined the location of the ETM in the Tamar estuary, which often was upstream of the salt limit. In contrast, Geyer et al. (1998) showed that lateral interactions between topography and flow maintain a pool of resuspendable particles, hence an ETM, well downstream of the salt limit in the Hudson River estuary. Particle trapping dynamics probably differ between estuaries or predominate at different times in the same estuary (e.g., spring tides versus neap tides).

In recent years the ecological role of ETMs in supporting anadromous fish recruitment also has been recognized (Dodson et al. 1989; Dauvin and Dodson 1990), and ETMs have been found to be areas of elevated zooplankton concentrations, especially the calanoid copepod *Eurytemora affinis* (Simenstad et al. 1994; Morgan et al. 1997; Kimmerer et al. 1998). It is believed that abundant food in the form of detritus, protozoa, and phytoplankton, in addition to the ETM particle trapping mechanisms described above, support the high zooplankton abundances. Immature and adult *Eurytemora* are important foods for larval and juvenile striped bass and white perch in Chesapeake Bay and other estuarine systems (Setzler-Hamilton 1991; Setzler-Hamilton and Hall 1991) establishing a potential trophic link that supports fish recruitment.

With the potential ecological role of ETMs and the new concepts of ETM particle trapping in mind, an interdisciplinary group of investigators undertook a new study of the Chesapeake Bay ETM in 1996. Under the aegis of the National Science Foundation Land Margin Ecosystem Research Program, Trophic Interactions in Estuarine Systems (TIES), we conducted a series of cruises in upper Chesapeake Bay to explore the ETM feature and biological production associated with it. Preliminary reports on these studies (Boynton et al. 1997; Roman et al. 1997) describe important linkages between physics, plankton biology, and production of young anadromous fish. More recent reports present additional information on anadromous fish recruitment (North and Houde 2001) and zooplankton (Roman et al. 2001). This paper presents an overview of the physics of the Chesapeake Bay ETM during 1996, with particular attention to its spatial and temporal variability, the factors that control particle trapping, and relationships between ETM processes and sedimentation in upper Chesapeake Bay.

Study Site

Earlier documentations (cited above) demonstrated that the ETM in Chesapeake Bay is contained within the uppermost part of the estuary (Fig. 1). Its location varies seasonally and at shorter time scales, but it is almost always found between latitudes 39°10′N and 39°28′N, a range of approximately 40 km. This region of the Bay has a mean volume of approximately 2.63 km^3 and a mean depth of approximately 4.1 m (Cronin 1971), not counting the small tributaries. It is incised by a narrow shipping channel maintained by dredging at a depth of approximately 12 m, which connects the Chesapeake and Delaware Canal with the Port of Baltimore and serves as the primary pathway for up-Bay salt intrusion. The average astronomical tidal range increases northward from 0.36 to 0.5 m, with typical maximum tidal current speeds of 0.5 m s^{-1} in the channel and 0.3 m s^{-1} over the broad shoals (Browne and Fisher 1988). Wind-forced water level fluctuations can be much larger than the astronomical tide (up to 1 m in range) due to the 2 d quarter-wave seiche response of the Bay to the passage of weather systems (Chuang and Boicourt 1989; Boicourt 1990), with associated current fluctuations of up to 0.2 m s^{-1} (Elliott et al. 1978). Net non-tidal gravitational circulation varies strongly in response to fluctuations in river flow (Elliott et al. 1978), and changes from a riverine, barotropic downstream flow above the limit of salt to a well-developed estuarine circulation below the limit of salt. Almost all of the freshwater flow enters from the Susquehanna River. At the average Susquehanna River flow of 1,100 m^3 s^{-1}, the freshwater replacement time of the ETM region of the Bay is approximately 1 mo.

More than 80% of the sediment entering the upper Bay comes down the Susquehanna River, with almost all of the rest resulting from shoreline erosion (Biggs 1970). The bottom sediments became gradually finer southward of the broad, sandy delta known as Susquehanna Flats (not shown in Fig. 1 due to sampling limitations), through short transition zones of silty sands and sandy silts, through the clayey silts that dominate

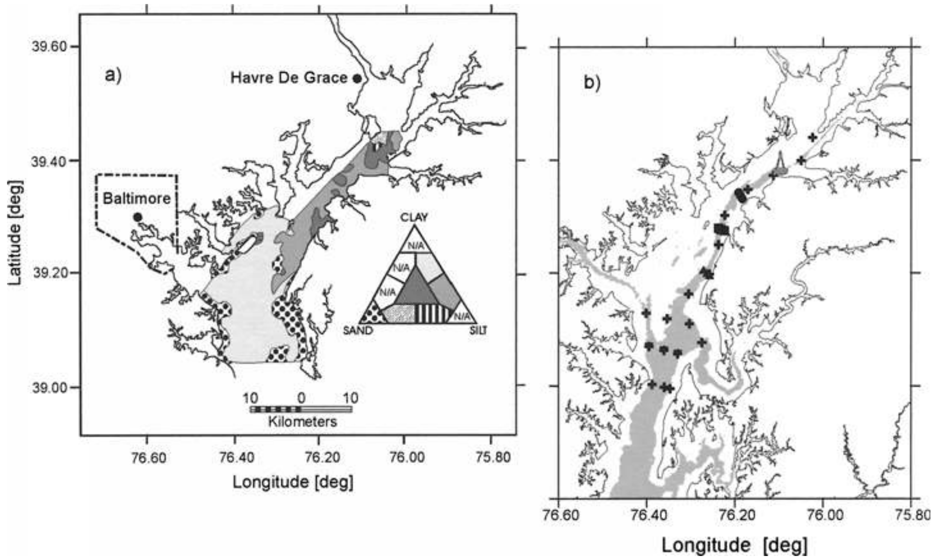

Fig. 1. a) Sediment distribution map of upper Chesapeake Bay (not including tributaries) using Shepard's tertiary classification scheme (Kerhin et al. 1988). Blank areas in tertiary diagram indicate a sediment type not present, and blank areas on the map in the main Bay indicate no sampling was done in that area. b) Map of upper Chesapeake Bay. Station locations for 1996: (✚) TIES CTD survey, (▲) ETM transect May 3–4, (●) ETM transect July 24–25, (■) ETM transect October 24–25. Buoy icon represents CBOS buoy location off Howell Point. Depths greater than 7 m are shaded.

the ETM region, to the silty clays that dominate the broad lower reach of the upper Bay. The deep channels of the upper Bay sediment rapidly (Officer et al. 1984) and require constant dredging to maintain navigable depths. Fringing sandy shelves in the broad lower reach reflect the importance of both wave-forced resuspension and shoreline erosion (Kerhin et al. 1988; Sanford 1994).

Suspended sediments are comprised of silts, clays, and aggregates thereof, with a low organic matter fraction (Schubel 1968a; Biggs 1970; Schubel and Kana 1972). Total suspended sediment (TSS) concentrations in the entire upper Bay are elevated relative to the rest of the estuary, with typical background concentrations of very slowly settling particles between 5–25 mg l^{-1} (Schubel 1968a,b, 1971; Sanford et al. 1991; Sanford and Halka 1993; Sanford 1994). These background particles tend to be uniformly distributed through the water column or slightly more concentrated in the lower water column, and they have a higher organic fraction than the particles that are resuspended from the bottom (Schubel and Biggs 1969). The ETM itself typically has TSS concentrations 20–100 mg l^{-1} higher than the background, with the largest concentrations resulting from tidal resuspension in near-bottom waters (Schubel 1968a,b). There is little spatial or temporal variation in dispersed (disaggregated) particle size distributions (Schubel 1968a; Schubel and Kana 1972), but aggregate sizes increase markedly at maximum tidal resuspension (Schubel 1971) and decrease slightly during periods of high riverflow (Schubel 1968a).

Methods

Five cruises were carried out in the upper Bay between February 1 and October 27, 1996, including two early hydrographic surveys of opportunity and three 5-d interdisciplinary TIES cruises. A total of 8 hydrographic (CTD) surveys of the upper Chesapeake Bay were made during these cruises. All surveys included 8–11 stations along the axis of the main (eastern) channel from just north of the Bay Bridge (approximately 39°00'N) to Turkey Point (approximately 39°26'N). The February 1 survey used the R/V *Kerhin* in conjunction with a Maryland Department of Natural Resources (MD-DNR) water quality sampling cruise after a late January flood event in the Susquehanna River basin. The March 15th survey used the R/V *Orion* and was funded by the Maryland Sea Grant Program. The remaining 6 surveys were conducted as part of three seasonal TIES cruises in 1996 on the R/V *Cape Henlopen*. Physical measurements during the TIES ETM cruises consisted of an initial CTD survey (Fig. 1), a 25-h CTD/ADCP lateral transect at the ETM location, a 25-h CTD/ADCP lateral transect at a location down-Bay from the ETM (Gibson Island transect), and a final CTD survey.

A SBE 25 Sealogger CTD was used for the February 1 and March 15 hydrographic surveys. The SBE 25 was equipped with an auxiliary 5-cm path-length transmissometer (SeaTech) as well as an

OBS-3 (Downing & Associates) backscatter sensor for measuring turbidity. The CTD was also outfitted with a well pump located at the same level as the turbidity sensors for collecting water samples in order to calibrate turbidity (NTUs) to TSS (mg l^{-1}). Additional auxiliary sensors included a PAR sensor, a dissolved oxygen (DO) sensor, and a fluorometer. The surveys began with a lateral transect near the Bay Bridge (3 stations) and then continued up the eastern channel of the Bay to the last station near Turkey Point. There were a total of 10 stations in these surveys, 8 of which were axial.

On the TIES cruises we used the R/V *Cape Henlopen* Neil Brown CTD mounted on a General Oceanics rosette, equipped with a 5-cm pathlength SeaTech transmissometer, a DO sensor, and a fluorometer. A well pump for collecting water samples was again attached to the CTD for calibration of the turbidity sensors. The first survey of each cruise (May 2, July 21, and October 22) began with a series of three lateral transects starting just north of the Bay Bridge and continued up-Bay to Turkey Point (Fig. 1). These surveys consisted of 18 total stations, 11 of which were axial. The location of the ETM was determined from an axial salinity and turbidity contour map of the initial CTD survey for each cruise, produced immediately after the survey was completed. The final survey of each cruise (May 6, July 25–26, and October 27) began at the northernmost station and proceeded down-Bay, omitting most of the lateral stations.

All CTD surveys followed the same protocols, paying particular attention to the turbidity sensors because of their importance for this study. Top to bottom CTD profiles were made at each station, making a special effort to sample as close to the bottom as possible (usually within 0.5 m). The lenses on the transmissometer were thoroughly cleaned with detergent and DI water prior to each hydrographic survey and open air and blocked path voltages were recorded for calibration. Water samples from the well pump were collected during CTD upcasts at locations and depths selected to cover the full range of turbidities encountered, and the times of the pumped samples noted for later calculation of turbidity calibration values from the transmissometer. Samples were collected in 250 ml Nalgene bottles and were kept refrigerated for laboratory TSS analysis.

TSS values (mg l^{-1}) were calculated from turbidity using a two step process. The voltage output of each transmissometer was calibrated to NTUs using a well-mixed laboratory Formazin turbidity standard. NTU values calculated from the field measurements were then converted to TSS by means of a calibration relationship derived for each cruise. The calibration relationship was derived by linear regression (sometimes in several parts) of water sample TSS values against NTUs from the transmissometer on the CTD. Water sample TSS analysis was performed by the Analytical Services Department at Horn Point Laboratory using standard methods (APHA 1975). Prewashed and weighed Whatman 24 mm (934-AH) filters, with 1.5 μm nominal pore size, were used for all TSS samples.

All CTD data were processed by bin averaging over 0.25 m depth bins using Seasoft software (Seabird Electronics, v. 4.216), correcting raw depths for instrumental and atmospheric pressure offsets. Salinity and TSS for individual transects were gridded and contoured using Surfer (Golden Software, v. 6.0). The data were gridded using the kriging algorithm with more weight given to points in the horizontal direction due to the asymmetric distribution of the data. The resulting distributions of salinity and TSS were used to estimate the positions of the limit of salt (defined as the intersection of the 1 psu isohaline with the bottom) and the center of the ETM (defined as the center of the region with near-bottom TSS concentrations more than 20 mg l^{-1} greater than background TSS concentrations). These position estimates are reported with a resolution of 1 km, accurate to approximately ± 2 km. This accuracy, which is better than the station spacing of 6 km, was derived by trying several different estimation techniques and noting the differences in position estimates.

Lateral transect time series stations were occupied for between 22–27 h during each cruise, running alternating Acoustic Doppler Current Profiler (ADCP) and CTD transects across the shipping channel near the center of the ETM. The ADCP (RD Instruments, 1.2 MHz Broadband) was mounted on an aluminum mast fixed to the port side of the vessel, with the transducer head submerged approximately 70 cm below the water surface. Current velocity profiles were collected in 50 cm bins from 2 m below the surface to within 1 m of the bottom. Ferrous metal on the ship can cause a directionally dependent offset in the internal ADCP compass, such that a heading correction for the ADCP was derived by comparing the heading from the ADCP compass to the ship's gyro at 10° increments around the compass. This heading correction had the form of a cosine function and was applied during post-cruise data processing.

A modified Owen settling tube (Valeport) was used to measure settling velocities of relatively undisturbed particles collected just above the bottom during each of the ETM lateral transects. The tube is approximately 5 cm in diameter by 1 m long. It is deployed horizontally in the water column at the desired depth and is oriented into the flow by a vane. A messenger is sent to close the ends of the tube, which is then raised back to the surface. On deck, the tube is placed vertically inside a water jacket and samples are withdrawn from the bottom for TSS analysis at specified, geometrically increasing time intervals. The water jacket, flushed with water at or very near the same temperature as the sample, is necessary to prevent convective cells from forming inside the settling tube. The sequence of bottom-withdrawal TSS values is analyzed using a spreadsheet implementation of the procedure described by Owen (1976). The product of this procedure is a settling velocity distribution of relatively undisturbed particles and aggregates.

Wind and salinity data were obtained from the northern bay Chesapeake Bay Observing System (CBOS) Buoy located off Howell Point at 39°22.5'N, 76°6.8'W. Susquehanna River discharge data from the gauging station at Conowingo Dam were obtained from the U.S. Geological Survey. Corresponding monthly and annual sediment load estimates were obtained from U.S. Geological Survey as well. These were derived using a new estimator model that optimizes estimates of average sediment load from average river discharge (Yochum 2000). Tidal height data for the Tolchester Beach, Maryland Station were obtained from the National Oceanic and Atmospheric Administration, National Ocean Service. Hourly tide data were 34 h low-pass filtered using a butterworth filter to reveal subtidal variability more clearly.

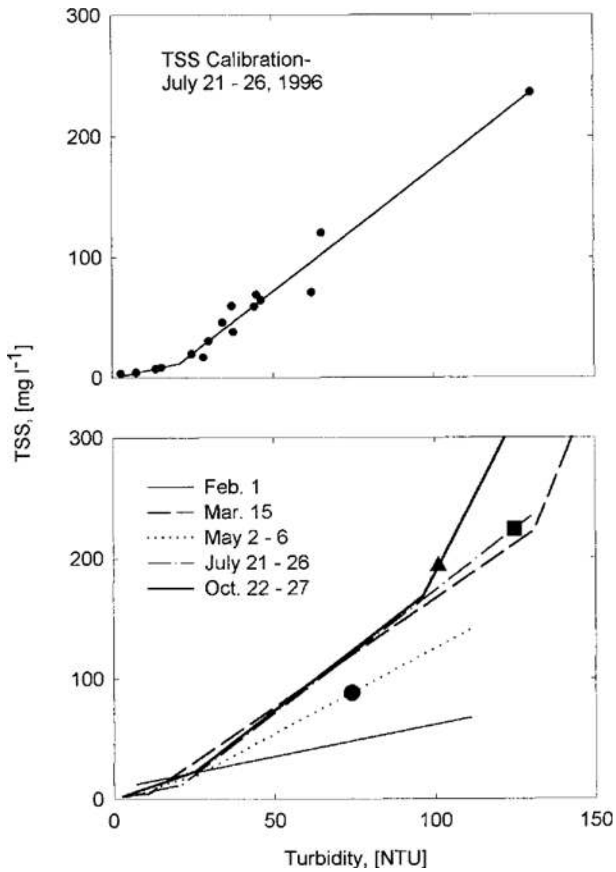

Fig. 2. Calibration of turbidity (NTU) from 5 cm pathlength tranmissometer to TSS (mg l^{-1}) from collected water samples. Upper panel shows example calibration curve from the July TIES cruise with fitted linear regression line (two part). Lower panel shows NTU to TSS regressions for all five 1996 cruises. Symbols indicate mean TSS concentration in Owen Tube samples from May (●), July (■), and October (▲) TIES cruises.

Results

Calibration of Turbidity to TSS

Derived calibrations between turbidity and TSS are shown in Fig. 2. An example of a single cruise calibration from July is shown in the upper panel, where the necessity for a two-part calibration is obvious. The slope of the calibration line at low concentrations is much lower than the slope at high concentrations. This is consistent with a two-part particle population consisting of fine, slowly settling particles that are nearly always in suspension and relatively large aggregates that are resuspended from the bottom and settle out of suspension rapidly. References cited above indicate that these two particle populations are always present in upper Chesapeake Bay. The increase in slope at 12 mg l^{-1} (approximately the background TSS concentration in July) is consistent with the response of transmissometers to larger particles (Baker and Lavelle 1984; note that their calibration plots have axes reversed relative to ours). A qualitatively similar calibration response was reported by Sanford (1994) for TSS collected in September 1992 in upper Chesapeake Bay. Two-part turbidity calibrations also were reported by Pak et al. (1988) and Downing and Beach (1989) in very different environments.

The lower panel of Fig. 2 shows the NTU-TSS calibration curves derived for all 5 ETM cruises in 1996. The calibration for the February 1 cruise is markedly different from the others. One line represents the entire calibration, with a slope similar to the low concentration slopes of the other calibrations. This implies that the suspended particles during the February cruise were relatively unaggregated fines. The May calibration slope was 270% higher than the February calibration slope at high concentrations, but only 70–80% as high as the slopes for the remaining cruises in the same range. At the very high TSS concentrations encountered near the bottom in March and October, third pieces of the calibration diagrams had to be

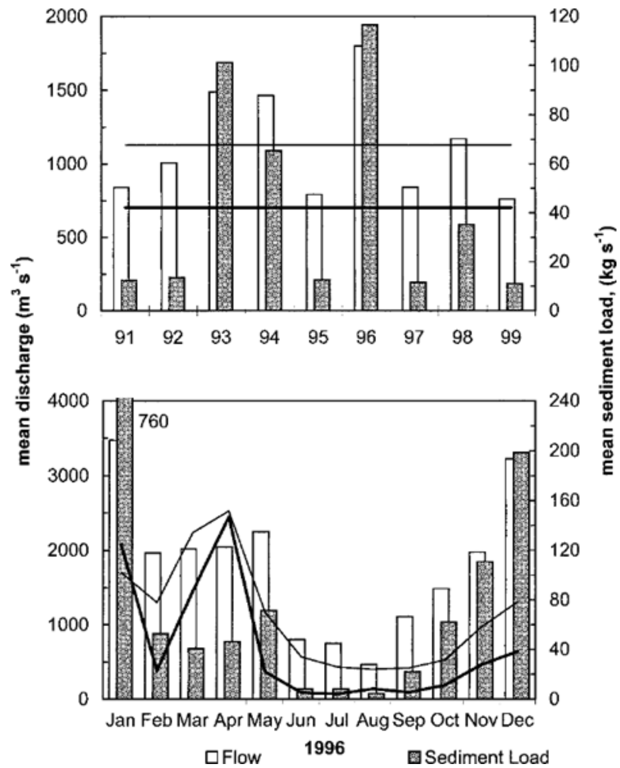

Fig. 3. Discharge and sediment load entering Chesapeake Bay from the Susquehanna at the Conowingo Dam gauging station. Upper panel shows annual means for individual calendar years from 1991 through 1999; means of discharge (———) and sediment load (▬▬▬) for entire 9-yr period are indicated. Lower panel shows monthly means for 1996 (bars) and monthly means for the 9-yr period (lines).

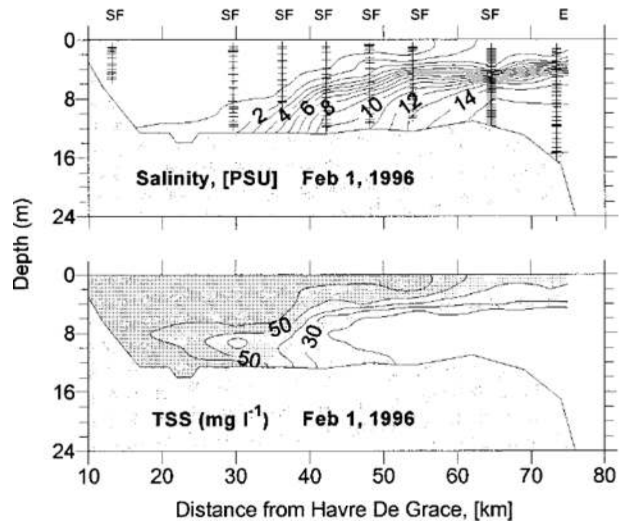

Fig. 4. Salinity and TSS contour plots of axial CTD surveys on February 1. Upper panel shows salinity (psu) contours and lower panels show filled TSS (mg l^{-1}) contours. Distance from head of bay at Havre De Grace (km) is shown on the abscissa. CTD data points (+) and phase of tide (F = flood, E = ebb, SF = slack before flood, and SE = slack before ebb) are indicated on the salinity contour plots.

added with even steeper slopes. The calibrations for each cruise were used to calculate TSS from turbidity for that cruise alone.

Susquehanna River Flow and ETM Particle Trapping

Calendar year averaged 1996 Susquehanna River flow and sediment load were the highest of the 9 years plotted in Fig. 3a. The 1996 average flow of 1,800 $m^3 s^{-1}$ exceeded the 9-yr average by 60% and the 1996 average sediment load exceeded the 9-yr average by 176%. The high annual average flow and sediment load were due to several factors. The most important by far was an enormous flood event during the last week of January, resulting from a record snowfall followed by a drenching rain. This flood resulted in approximately 9×10^9 m^3 of freshwater and 1.5×10^9 kg of sediment entering the Bay from the Susquehanna River in approximately 2 wk (Zynjuk and Majedi 1996). The highest flow rates were approximately 10 times the January average flow and the total sediment loading was approximately 17 times the total for an average January. Flow and sediment loading during the rest of the winter, spring, and most of the summer were not remarkably different from average conditions, with 20% higher freshwater flow and 20% lower sediment loading (Fig. 3b). A difference in 1996 was that the winter-spring freshet was spread out uniformly during the months of February–May, rather than peaking in March and April as usual. The last 4 mo of 1996 were much wetter than usual with 140% higher freshwater flow and 370% higher sediment loads than average.

Figure 3a and b are plotted such that flow and sediment loading bars of equal height would correspond to a monthly average TSS concentration of 60 mg l^{-1} in inflowing Susquehanna River waters. The bars are seldom of equal height, however, reflecting the nonlinear relationship between flow and sediment loading of the Susquehanna basin. Low flows yield very low sediment loads, and high flows yield very high sediment loads. Inflowing Susquehanna TSS concentrations averaged 219 mg l^{-1} in January 1996, 20 mg l^{-1} in March, 32 mg l^{-1} in May, 11 mg l^{-1} in July, and 42 mg l^{-1} in October. The average for 1996 was 65 mg l^{-1}.

Axial distributions of salinity and TSS observed on February 1, at the tail end of the January flood, are shown in Fig. 4. These represent the most extreme TSS distributions observed in 1996. On February 1, the January flood appeared to have changed the upper Bay from a partially mixed estuary into a salt wedge estuary. Freshwater was be-

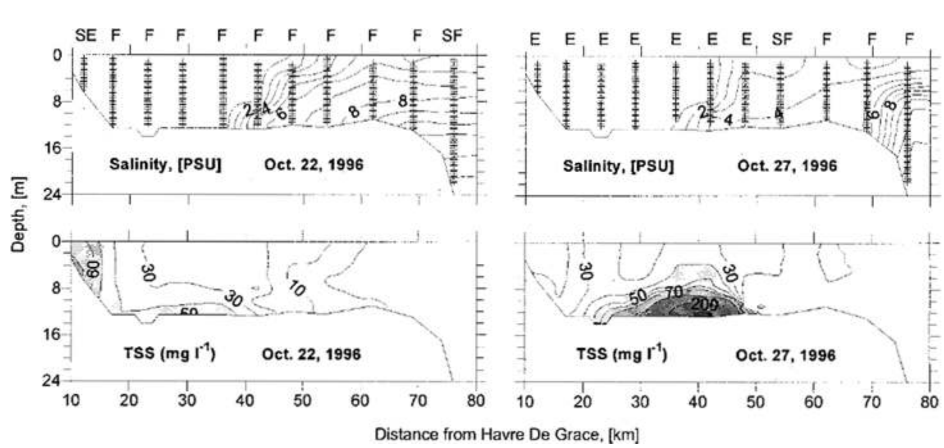

Fig. 5. Salinity and TSS contour plots of axial CTD surveys on October 22 (left) and October 27 (right), as in Fig. 4.

ing advected seaward in a thin lens overlying a very sharp pycnocline at 4–6 m depth. TSS concentrations of 30–60 mg l^{-1} were being carried seaward in this fresh surface layer. The initial surge of the flood from January 20–22 may have pushed salt out of the upper Bay, but if so the salinity structure had rebounded strongly by February 1. The result was an intrusion of salt water more pronounced than any other we observed in 1996. The lower layer was relatively clear, except for a weak ETM-like near-bottom TSS maximum between kilometers 14–30 near the limit of salt. The majority of the flood sediments appear to have been escaping the upper Bay, at least over the channel. There were no current data collected during this period, so direct estimates of sediment transport rate were not possible. The turbid surface layer was deeper than the average depth of the ETM zone, such that sediment may have been deposited over the shallow shoal areas adjacent to the channel. Sediment cores were collected in 8 different locations on February 1 and March 13, and they failed to identify any clear evidence of newly deposited flood sediments (Halka unpublished data).

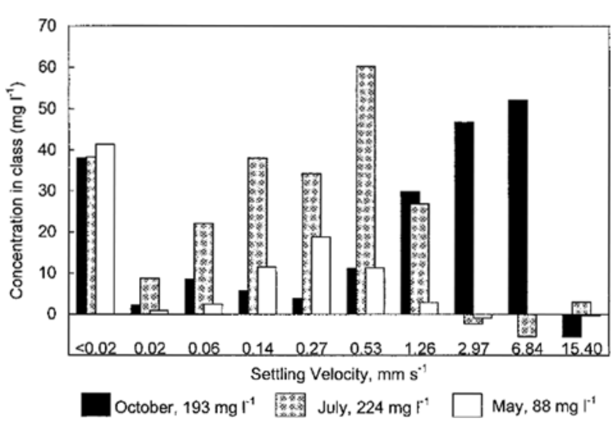

Fig. 6. Settling velocity distributions from modified Owen Tube casts on May, July, and October TIES cruises. All casts were taken near bottom, in the area of the ETM, during the ETM lateral transect. Slightly negative values at high settling velocities indicate errors in sample collection or analysis, or the accumulated error of the numerical analysis.

In contrast to the fate of the January flood, the October 22 and 27 surveys presented in Fig. 5 show a case of what appears to be very efficient ETM sediment trapping. Heavy rains in the upper part of the Susquehanna watershed several days prior to the first survey resulted in a large pulse of freshwater flow that peaked at just over 5,000 $m^3 s^{-1}$ on October 21 and 22. The October 22 survey caught this inflow and its associated sediment load as they entered the upper part of the ETM zone. Although a weak ETM was centered at km 30, just above the limit of salt, the highest TSS concentrations were distributed nearly uniformly through the water column above km 20 in the inflowing freshwater. On October 27, the salt content of the upper Bay was markedly lower, though the limit of salt was at almost the same location as on October 22. TSS concentrations above km 20 had fallen to background levels, but a pronounced ETM was centered at km 41 with near-bottom TSS concentrations $>$ 500 mg l^{-1}. It is quite likely that this large pool of suspended solids in the lower layer of the channel resulted from direct trapping of the high sediment loads entering the Bay a few days before.

The obvious question is why the massive January flood sediment load appears to have largely escaped the ETM, but the October storm sediment load appears to have been efficiently trapped. The likely answer is shown in Fig. 6, which summarizes the results of settling tube experiments carried out during each of the three TIES cruises. These results are presented in terms of the TSS concentration in each of 10 settling velocity classes. All three settling samples were drawn from relatively high

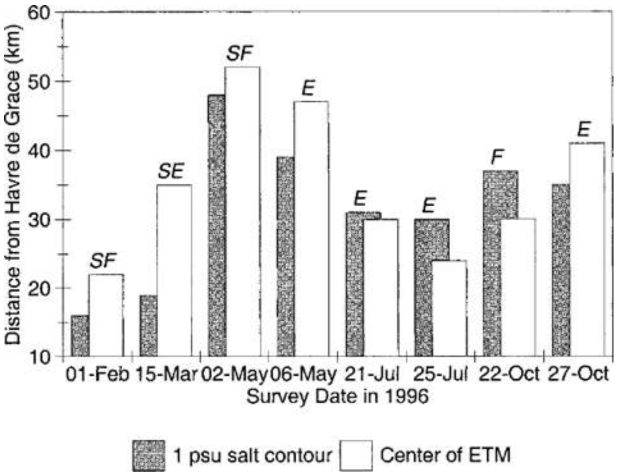

Fig. 7. Relative position of the 1 psu isohaline and the center of the ETM for the eight surveys made in 1996. Phase of tide (F = flood, E = ebb, SF = slack before flood, and SE = slack before ebb) at station closest to the ETM is indicated.

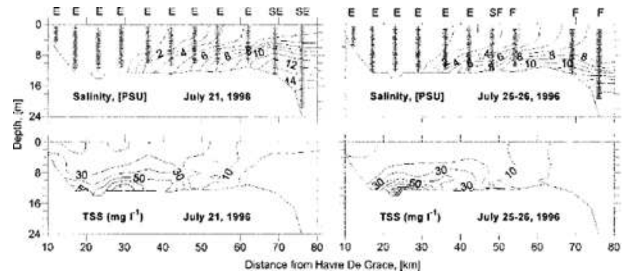

Fig. 8. Salinity and TSS contour plots of axial CTD surveys on July 21 (left) and July 25–26 (right), as in Fig. 4.

TSS concentration near-bottom water at the center of the ETM, and all three had approximately the same concentration of background TSS (settling slower than 0.02 mm s^{-1}). Discounting this very slowly settling material, the May and July samples had approximately the same median settling speed (0.3 mm s^{-1}), while the October sample had an order of magnitude higher median settling speed (3 mm s^{-1}). Referring to Fig. 2, at the concentration of the settling tube samples the slopes of the calibration lines increased slightly from May to July and more than doubled to October. The implication is that the October sample contained larger particles that settled at much higher rates than either the May or July sample. By extension, the February TSS must have been relatively fine material, settling at much slower rates than in any of the other surveys. We infer that the January flood sediment load escaped the ETM because it settled too slowly and the October storm sediment load was efficiently trapped because it settled quite rapidly (but not rapidly enough to deposit before it reached the ETM).

Covariability of the ETM and the Limit of Salt

From the example salinity-TSS distributions presented in Figs. 4 and 5, it is apparent that the ETM in upper Chesapeake Bay tended to be associated with the limit of salt intrusion. It is also apparent that this association was not perfect. The center of the ETM was approximately 7 km up-Bay of the limit of salt on October 22, but 6 km down-Bay of the limit of salt on October 27. This cannot be explained by the tidal resuspension lag discussed by Dyer and Evans (1989) for which the limit of salt would lead the ETM in the direction of tidal flow. In the present examples, the opposite was true; the limit of salt appears to have lagged behind the ETM in the direction of tidal flow in both surveys.

In order to investigate the covariability of the ETM and the limit of salt further, we estimated the position of both for all 8 axial surveys carried out in 1996 (Fig. 7). The results show that the two tended to covary on a seasonal basis. On average, the limit of salt was 3 km upstream of the ETM. The limit of salt responded as would be predicted based on the pattern of monthly averaged freshwater flows (Fig. 3). It was further down-Bay in high flow months and further up-Bay in low flow months, with the exception of the February 1 survey after the January flood (discussed above). The center of the ETM and limit of salt were usually not coincident. The average difference between the two was 7 km, approximately the same as a typical tidal excursion in the upper Bay, but the direction of the difference was unrelated to the phase of the tide during the survey. If the ETM was caused by the convergence of the gravitational circulation alone, it would always be coincident with the limit of salt. As stated above, a tidal resuspension lag alone would result in the salt limit always leading the ETM in the direction of the tidal flow. Neither of these predictions is borne out by the data, but why?

The answer is likely related to daily or weekly variability of ETM dynamics caused by fluctuations in freshwater flow, sediment loading, and atmospheric forcing, variability that was imperfectly resolved by our sampling scheme. The beginning and ending surveys from the July cruise (Fig. 8) illustrate the consequences of this variability. On July 21 the center of the ETM and the salt limit were nearly coincident at km 30 on an ebb tide. On July 25–26 the limit of salt was in almost the same location, but the center of the ETM was 6 km further upstream, again on an ebb tide.

Fortunately, a CBOS mooring was in place on

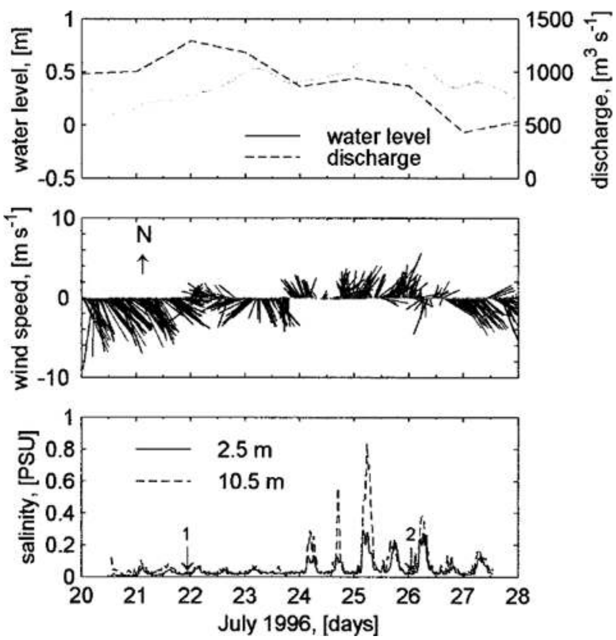

Fig. 9. Tide, river discharge, wind, and salinity time series for July cruise. Upper panel: 34 h low-pass filtered water level, in meters above MLLW, for hourly tide data from Tolchester Beach, Maryland. The daily discharge from the Susquehanna River through the Conowingo Dam is also shown. Middle panel: vector plot of winds (oceanographic convention) from CBOS buoy near Howell Point. Lower panel: salinity time series from the upper (2.5 m) and lower (10.5 m) current meters at CBOS buoy site; times of passage of initial and final CTD surveys are indicated by (1), and (2), respectively.

the eastern side of the channel at km 20 throughout this time period, with current meters and T/C sensors at 2.5 and 10.5 m depth and an anemometer at 3 m above the water surface. The salinity time series from this mooring, wind, low-pass filtered water level at Tolchester, and daily Susquehanna River flow are shown in Fig. 9. Between the two surveys it appears that the limit of salt had moved upstream to almost km 20 (note the salinity of 0.8 at 10.5 m depth on July 25) and was in the process of moving back downstream when it was observed early on the morning of July 26. The exact cause of this short term intrusion and retreat is not obvious. It may have been a delayed depth-dependent response to southward winds before July 24 followed by northward winds from July 24–26. It may have resulted from the barotropic filling and emptying of the upper Bay apparent as the low frequency rise in water level that peaked on July 25 and began falling on July 26. It may have been associated with the decreasing Susquehanna River flow starting on July 22. It may have been some combination of all of the above. It is apparent that the limit of salt moved up the channel and back approximately 10 km over a 4–6 d period. Significant non-tidal current fluctuations in this same period band were reported by Elliott et al. (1978) from a mooring at the same location.

This rapid non-tidal movement of the salt front, when added to or subtracted from regular tidal movement, most likely led to the observed separations of the ETM and the salt limit. The mechanism was most probably a suspended sediment transport lag, consisting of both a resuspension lag (due to the finite bottom stress required to erode deposited sediments and the finite upward mixing time of eroded sediments) and a transport lag (due to the preferential concentration of rapidly settling ETM particles near the bottom in slower moving water). The salt limit and the ETM started out together on July 21. The salt limit moved rapidly up the Bay from July 22–25 and the ETM followed behind. The salt limit subsequently began to move back down-Bay to its July 21 location, once again leaving the ETM behind but now in an up-Bay direction. Our surveys caught two snapshots of a continuously and rapidly changing environment, rather than two steady-state distributions.

Temporal Variability at the ETM Center

The full spatial and temporal variabilities of the 25-h lateral transect time series observations during each of the TIES cruises are too complex to discuss in this overview paper. Suffice it to say here that we observed significant lateral variability associated with the changing phases of the tide and the steep channel-shoal topography, that undoubtedly play a role in channel-shoal exchange processes. We believe that axial dynamics in the channel dominate particle trapping processes in the Chesapeake Bay ETM because the ETM is so clearly associated with the limit of salt and because salt transport is primarily confined to the axial channel. We present and discuss only the time series from the center channel station of the lateral transect carried out on October 24–25, 1996 (Fig. 10). This transect was chosen because, on average, it was situated almost exactly at the limit of salt.

The time series began as ebb tide was decreasing towards slack before flood. The water column was unstratified and nearly fresh, since the salt limit was almost at its maximum down-Bay excursion. As the tide turned and flooded, the salt limit was advected past the transect location as a sharp near-bottom front. At slack before ebb near-bottom salinities were > 4 in a thin bottom mixed layer beneath a sharp pycnocline. The upper water column remained unstratified and nearly fresh. The salt limit was advected down-Bay past the transect location on the succeeding ebb tide. The entire sequence was repeated one more time before the end of the time series.

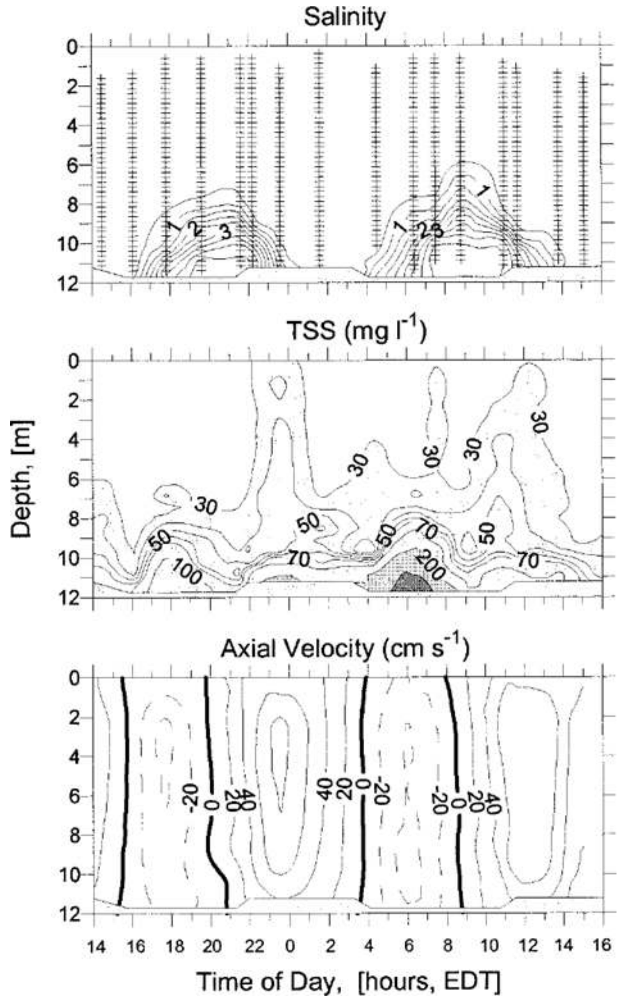

Fig. 10. Time-depth contours of salinity, TSS, and along-channel currents from the ETM channel station on October 24–25. Upper panel: salinity contours (psu). Middle panel: filled TSS contours (mg l^{-1}). Salinity and TSS are from CTD casts taken at the center channel station during the ETM lateral transect. CTD data points are indicated by (+). Lower panel: along channel currents (projected angle = 195°, cm s^{-1}) from successive ADCP passages across the channel station. Positive velocities (——) are ebb and negative velocities (▬▬) are flood.

The stratification variations imposed by the passage of the salt limit had clear consequences for sediment resuspension and velocity shear. Local resuspension is most clearly indicated by near-bottom increases and decreases of TSS in phase with the near-bottom velocity. Local resuspension was quite pronounced at maximum flood tide and much weaker at maximum ebb tide. Upward mixing appeared to have been limited by the pycnocline. Though it is possible that some of the TSS high in the water column at maximum ebb resulted from upward mixing through the pycnocline, it is more likely that this material resulted from resuspension upstream, rapid downstream advection by the strongly sheared ebb currents, and rapid diffusion through the well-mixed upper water column. The slightly elevated above-pycnocline TSS concentrations on flood are probably the remnant of this material. Stratification and gravitational circulation near the salt limit affected the observed velocity structure by increasing vertical shear and raising the height of the velocity maximum on ebb, while decreasing vertical shear and lowering the height of the velocity maximum on flood. This pattern is most obvious in the ebb at 00:00 on October 25 and the flood at 06:00 on October 25. The gravitational circulation also caused the near-bottom currents to turn to flood sooner and to ebb later than the near-surface currents.

Discussion

While the results presented here confirm the basic descriptions of the Chesapeake Bay ETM offered by Schubel (1968a,b) and Schubel and Pritchard (1986), they refute the idea that the convergence of the gravitational circulation is primarily responsible for its formation, with tidal resuspension merely modulating TSS concentrations (Schubel 1968a,b; Festa and Hansen 1978; Officer 1980). If this earlier explanation was correct, then the ETM would not become separated from the limit of salt, as we observed. The range of particle settling speeds trapped by the gravitational circulation in the model of Festa and Hansen (1978) was 10–100 times smaller than the settling speeds we observed. The highest settling speeds trapped in Geyer's (1993) improved ETM model combining gravitational circulation with stratification damped mixing (but no tidal currents) are at the low end of the range of our observations as well.

Our data indicate that asymmetrical tidal resuspension and asymmetrical tidal transport of rapidly settling aggregates are primarily responsible for the Chesapeake Bay ETM, as illustrated schematically in Fig. 11. Tidal suspended sediment transport is biased in a net downstream direction above the limit of salt and in a net upstream direction below the limit of salt, leading to the formation of a pool of resuspendable particles near the limit of salt. The axial convergence of the gravitational circulation and the associated salinity structure near the limit of salt are the major causes of these tidal asymmetries, but without tidal resuspension the rapidly settling aggregates would likely remain on the bottom where they were initially deposited, the concentrated pool of resuspendable particles would not be formed, and the ETM as such would either not exist or be greatly weakened. The resuspendable particle pool lags behind the motion of the salt limit because of the resuspension lag described by Dyer (1988) and because the near-bottom center of mass of the rapidly settling suspended particles moves more slowly than the water above it. The wind-forced separation of the ETM and salt limit shown in Fig. 11 is similar to the freshwater flow lags of the ETM behind the salt limit observed in the Tamar and Weser estuaries by Grabemann et al. (1997).

This explanation of the Chesapeake Bay ETM is also more in line with recent explanations of ETM formation in other estuaries. In almost every case, a spatially limited pool of resuspendable particles is the key factor. The mechanisms responsible for formation of this particle pool vary from estuary to estuary, sometimes depending on nonlinear tidal pumping (Jay and Musiak 1994; Uncles et al. 1998; Brenon and Le Hir 1999; Guezennec et al. 1999), sometimes on a tidal resuspension lag (Dyer 1988; Dyer and Evans 1989; Hughes et al. 1998), sometimes on tidally induced topographic trapping or tidally varying channel-shoal exchange (Geyer et al. 1998), etc. In partially mixed estuaries like Chesapeake Bay, asymmetric tidal transport near the limit of salt is often the responsible mechanism (Hamblin et al. 1988; Burchard and Baumert 1998), but the convergent circulation and associated salinity structure that cause the tidal asymmetries are specific contributing factors, not universal requirements for ETM formation. Indeed, the 1999 Chesapeake Bay ETM structure reported by North and Houde (2001) is below the limit of salt and appears to be closely associated with rapidly changing topography near the upper end of the ETM zone.

Given our emphasis on tidal asymmetry, a discussion of its effects on our survey data and ETM position estimates is appropriate. There are essentially three effects. First, the phase of the tide should affect the amount and location of resuspended sediment in the water column, as illustrat-

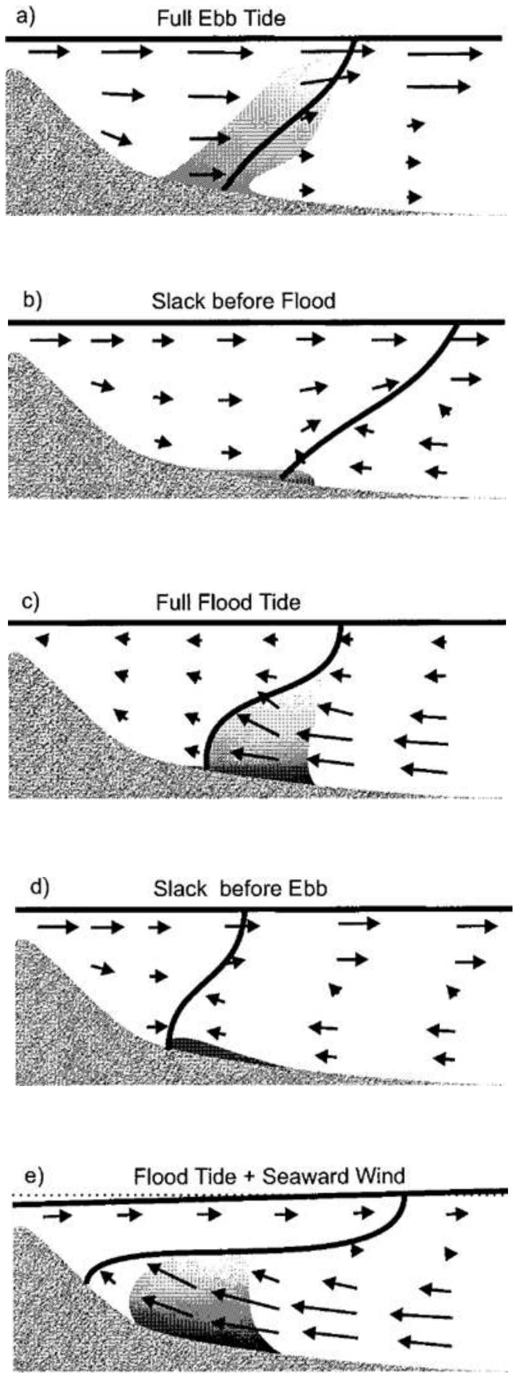

Fig. 11. Conceptual diagram of particle trapping in the Chesapeake Bay ETM. The river is to the left and the sea is to the right. The heavy curved line represents the 1 psu isohaline, the arrows represent current vectors, and the shading represents suspended sediment. The strength of the gravitational circulation (GC) is exaggerated for purposes of illustration. a) At full ebb tide, the GC enhances ebb currents upstream of the salt front, resulting in resuspension of sediments and zooplankton high into the unstratified water column and advection downstream above the pycnocline. Some settling through the pycnocline occurs. The GC opposes ebb currents below the salt front, such that only settling occurs. b) At slack before flood,

←

only the GC remains and previously resuspended sediments have settled to the bottom. Stratification is maximum below the salt front. c) At full flood tide, the GC enhances flood currents below the salt front and causes resuspension of sediments, but only to the height of the pycnocline. The GC opposes flood tidal currents above the salt front, with no resuspension. d) At slack before ebb, only the GC remains and previously resuspended sediments have settled to the bottom. Stratification is minimum. e) A seaward wind circulation added to flood tidal currents and the GC further enhances resuspension below the salt front, but it also moves the toe of the salt front landward faster than the ETM and results in a temporary separation between salt and suspended sediments. The enhanced lower layer circulation is lagged behind the onset of the wind by the time required to establish an opposing surface slope in the upper Bay.

ed in Fig. 11. Second, tidal straining of the density structure should result in changes in the slope of the salt front, also as illustrated in Fig. 11. Third, tidal resuspension lags should result in the ETM lagging the salt front, remaining slightly seaward at the end of flood and slightly landward at the end of ebb. There are some indications of these effects in the surveys presented here. The ebb tide surveys of July 21 (Fig. 8) and October 27 (Fig. 5) show higher concentrations distributed throughout the water column upstream of the salt front and extended slightly downstream in the surface layer, as in panel a of Fig. 11, although the expected intratidal differences are overwhelmed by differences in freshwater flow, sediment loading, wind forcing, and tidal current strength between the surveys. In fact, in five out of the eight cases shown in Fig. 7, correcting for the expected tidal lags would increase the separation between the ETM and the salt limit rather than decrease it. Tidal effects are important at intratidal time scales (Fig. 10), but longer-term, larger scale effects dominate over times scales of days to months.

The residence time of terrestrial particles in the ETM pool must be finite, or ETM TSS concentrations would continually increase. In some estuaries (e.g., the Columbia River), the ETM represents a delay between the delivery of terrestrial material from the river and its ejection to the coastal ocean, with little net accumulation in the bottom sediments (Crump and Baross 1996). In others, accumulation in the sediments and accretion of the bottom is the ultimate fate of terrestrial material. There is abundant evidence that sedimentary accumulation dominates in Chesapeake Bay. The upper Bay is shoaling at a much higher rate than the mid-Bay (Officer et al. 1984; Colman et al. 1992). Estimates range between 0.3–1.2 cm yr^{-1} (Officer et al. 1984; Kerhin et al. 1988; Donoghue et al. 1989; Halka unpublished data). Other estimates indicate that the ETM region of Chesapeake Bay permanently traps between 70% (Biggs 1970; Schubel and Pritchard 1986) and 100% (Donoghue et al. 1989) of the terrestrial material delivered from the Susquehanna River. Exactly when and how permanent sedimentation occurs is not known, but we speculate that spring-neap variability in tidal currents may be an important factor in the ETM channel. All of the 1996 TIES ETM cruises were designed to be centered around spring tides, when tidal currents and tidal resuspension were at a maximum. Neap tidal currents in the upper Bay are approximately 30% weaker than spring tidal currents. This may be just enough of a decrease in energy to allow a substantial portion of the resuspendable particle pool to consolidate, resist subsequent erosion, and be buried under newly delivered material. Over the shoals, net sedimentation is more likely controlled by the timing between delivery events and wave-forced erosion events (Sanford 1994).

Sedimentation rates in the ETM shipping channels are remarkably high compared to the adjacent shoals, where all of the upper Bay sedimentation rates cited just above were collected. It is not possible to estimate sedimentation rates in dredged shipping channels by conventional means, but the dredging records themselves may be used to obtain an approximate value. Annual maintenance dredging records from the upper 48 km of the shipping channel leading from Baltimore to the Chesapeake and Delaware Canal (27 km of which form the channel of the upper part of the ETM zone) have been compiled by the Maryland Geological Survey since 1986 (Panageotou et al. 1998). The authorized width of the channel is 137 m, which gives a total sediment surface area of 6.6×10^6 m^2. The annual average dredged volume is 1.1×10^6 m^3, which gives an annual average sedimentation of 17 cm, 14–55 times the annual sedimentation rate on the adjacent shoals. This focusing of sedimentation into the channel may be due to redistribution from the shoals to the channel by storm events (Sanford 1994), focusing of initial deposition into the channel by unknown lateral transport processes, or up-Bay transport of material from below the ETM zone. We also note that there is an apparent correlation between annual fluctuations in sediment loading from the Susquehanna and maintenance dredging volume during the following winter (not shown), implying that the focusing process may occur quickly.

Two of our important results are related to sediment settling velocities; settling velocities of resuspended TSS from the Chesapeake Bay ETM were high relative to the settling velocities of disaggregated silt and clay particles, and settling velocities of ETM particles increased significantly from February through May and July to October. Both results were based primarily on settling velocity distributions measured using a modified Owen settling tube, in combination with changes in the turbidity-TSS calibration relationships. There have been questions raised in the literature about the accuracy and repeatability of the settling tube technique, which we would be remiss to ignore. Dearnaley (1997) showed that floc break-up, re-flocculation, and internal circulation within a settling tube had the net result of reducing settling speed estimates relative to direct video techniques. Dyer et al. (1996) also indicated that, relative to video techniques, settling tubes tended to underestimate settling velocities, though careful control of sampling protocols gave comparable results between different tube designs. Hill and Milligan (1999) argued that the artifacts induced by floc breakup and reflocculation can explain the apparent concentration dependence of settling velocity as observed in settling tube measurements (Burt 1986).

While we cannot state categorically that these problems did not affect our measurements, there are several factors that indicate such problems may not have been as serious in our case, or at least that the settling effects that we observed were qualitatively correct. First, we observed internal circulations in our settling tube experiments in previous trials, that were related to convection caused by temperature differences between the sample and the external environment. We devised our temperature control water jacket to minimize this problem, and did not use any data from experiments with visible convection cells. Internal circulation tends to homogenize the sediment suspension inside the tube, lowering the median settling velocity estimate, which may explain some of the effect described by Dyer et al. (1996). It is also possible that the video techniques that give higher median settling speeds do not resolve the fine, slowly settling fraction of the particle population, such that videographic median settling speeds are biased upward. We did not observe a concentration dependence of settling speed in our samples; two samples at almost the same concentration (October and July) had very different settling velocity distributions, while two samples at very different concentrations (May and July) had very similar median settling velocities. The relative differences between our samples cannot be due to a bias introduced by different initial TSS concentrations. The relative settling speeds of our samples are consistent with the relative slopes of the accompanying turbidity-TSS calibration lines, assuming that more rapidly settling particles represent larger aggregates of similar composition. We have found in previous modeling work that a settling velocity of approximately 1 mm s^{-1} is required to match observed resuspension-deposition cycles in upper Chesapeake Bay (Sanford and Halka 1993; Sanford and Chang 1997), very close to the average of the three settling velocities quoted here.

We believe that the median settling velocities determined from our settling tube measurements are reasonable, that the relative increase in settling velocity from May to October is real, and that the implied lower settling velocity of the January flood material is real. Such seasonal changes in settling speed have important consequences. They may explain why there was very little evidence of sediment trapping in the Chesapeake Bay ETM following the January 1996 flood, while Hurricane Agnes in June 1972 left approximately 75% of its sediment load in the ETM zone in a layer approximately 0.2 m thick (Schubel and Pritchard 1986). The relatively efficient trapping after Agnes may have been because particles were more highly aggregated and settled more rapidly. We will never know if this is true, but it is plausible and implies that the sedimentological consequences of major events may depend on when they occur.

Seasonal changes in settling speed are most probably due to biogenic changes in the stickiness or packaging of the aggregates. Schubel and Kana (1972) found that zooplankton fecal pellets were important agents of particle agglomeration in upper Chesapeake Bay, and zooplankton activity is clearly seasonal. Jahmlich et al. (1999) also found increasing aggregate size related to transparent exopolymer particles and bacterial cell abundance in the bottom boundary layer of a bight of the Baltic Sea, and Zimmermann-Timm et al. (1998) found that the largest aggregates in the Elbe Estuary occurred in spring and summer in association with high particle-attached microbial activity. Data obtained at the mouth of the Susquehanna River for the U.S. Environmental Protection Agency Chesapeake Bay Monitoring Program indicate seasonal increases of approximately 50% in DOC concentrations between the winter/early spring and the summer/fall during 1994 and 1995. Increased organic loading and increased microbial activity might both lead to increased particle stickiness and increased aggregation.

We acknowledge that our results are tantalizing but preliminary. We have attempted to construct a plausible scenario for the controlling physics of the Chesapeake Bay ETM based on data that is intriguing but limited. We have suggested and discussed specific physical mechanisms that are consistent with the data and more in keeping with recent understanding than previous ideas. We have not tried to prove these suggested mechanisms or explore them quantitatively—to do so would have been to push the data set beyond its limits.

Acknowledgments

We gratefully acknowledge the support of the National Science Foundation through Grant No. DEB-9412113. We also thank W. C. Boicourt for the Howell Point CBOS buoy data, S. Yochum for the Susquehanna sediment load data, and J. Hagy for providing Susquehanna dissolved organic carbon concentration data culled from the U.S. Environmental Protection Agency Chesapeake Bay Program data base. We thank two anonymous reviewers for their helpful suggestions for improving the paper. Finally, our thanks go to the crews of the R/Vs *Kerhin, Orion,* and *Cape Henlopen* for their help during the field work. This is University of Maryland Center for Environmental Science publication no. 3469.

Literature Cited

APHA. 1975. Standard Methods for Examination of Water and Wastewater. American Public Health Association, Washington, D.C.

Baker, E. T. and J. W. Lavelle. 1984. Effect of particle size on the light attenuation coefficient of natural suspensions. *Journal of Geophysical Research* 89:8197–8203.

Biggs, R. B. 1970. Sources and distribution of suspended sediment in northern Chesapeake Bay. *Marine Geology* 9:187–201.

Boicourt, W. C. 1990. The influences of circulation processes on dissolved oxygen in Chesapeake Bay, p. 1–59. *In* D. E. Smith, M. Leffler, and G. Mackiernan (eds.), Oxygen Dynamics in Chesapeake Bay, A Synthesis of Recent Research. Maryland Sea Grant, College Park, Maryland.

Boynton, W. R., W. Boicourt, S. Brandt, L. Harding, E. Houde, D. V. Holliday, M. Jech, W. M. Kemp, C. Lascara, S. D. Leach, A. P. Madden, M. Roman, L. Sanford, and E. M. Smith. 1997. Interactions between physics and biology in the estuarine turbidity maximum (ETM) of Chesapeake Bay, USA. CM. 1997/S:11. International Council for the Exploration of the Sea, Copenhagen, Denmark.

Brenon, I. and P. Le Hir. 1999. Modelling the turbidity maximum in the Seine estuary (France): Identification of formation processes. *Estuarine Coastal and Shelf Science* 49:525–544.

Browne, D. R. and C. W. Fisher. 1988. Tide and Tidal Currents in the Chesapeake Bay. National Oceanic and Atmospheric Administration, Rockville, Maryland.

Burchard, H. and H. Baumert. 1998. The formation of estuarine turbidity maxima due to density effects in the salt wedge. A hydrodynamic process study. *Journal of Physical Oceanography* 28:309–321.

Burt, T. N. 1986. Field settling velocities of estuary muds, p. 126–150. *In* A. J. Mehta (ed.), Estuarine Cohesive Sediment Dynamics. Springer-Verlag, Berlin.

Chuang, W.-S. and W. C. Boicourt. 1989. Resonant seiche motion in the Chesapeake Bay. *Journal of Geophysical Research* 94: 2105–2110.

Colman, S. M., J. P. Halka, and C. H. Hobbs, III. 1992. Patterns and rates of sedimentation in Chesapeake Bay during holocene rise in sea level, p. 101–111. *In* C. H. Fletcher and J. F. Wehmiller (eds.), Quaternary Coastal Systems of the United States. Society of Economic Paleontologist and Mineralogists. Special Publication no. 48. Society for Sedimentary Geology, Tulsa, Oklahoma.

Cronin, W. B. 1971. Volumetric, Areal, and Tidal Statistics of the Chesapeake Bay Estuary and Its Tributaries. The Chesapeake Bay Institute of the Johns Hopkins University, Baltimore, Maryland.

Crump, B. C. and J. A. Baross. 1996. Particle-attached bacteria and heterotrophic plankton associated with the Columbia River estuarine turbidity maxima. *Marine Ecology Progress Series* 138:265–273.

Dauvin, J. C. and J. J. Dodson. 1990. Relationship between feeding incidence and vertical and longitudinal distribution of rainbow smelt larvae (*Osmerus mordax*) in a turbid well-mixed estuary. *Marine Ecology Progress Series* 60:1–12.

Dearnaley, M. P. 1997. Direct measurement of settling velocities in the Owen Tube: A comparison with gravimetric analysis, p. 75–85. *In* W. R. Parker, R. Parker, and J. Watts (eds.), Cohesive Sediments. John Wiley and Sons, New York.

Dodson, J. J., J. C. Dauvin, R. G. Ingram, and B. d'Anglejan. 1989. Abundance of larval rainbow smelt (*Osmerus mordax*) in relation to the maximum turbidity zone and associated macroplanktonic fauna of the middle St. Lawrence Estuary. *Estuaries* 12:66–81.

Donoghue, J. F., O. P. Bricker, and C. R. Owen. 1989. Particle-borne radionuclides as tracers for sediment in the Susquehanna River and Chesapeake Bay. *Estuarine, Coastal and Shelf Science* 29:341–360.

Downing, J. P. and R. A. Beach. 1989. Laboratory apparatus for calibrating optical suspended solids sensors. *Marine Geology* 86: 243–249.

Dyer, K. R. 1988. Fine sediment particle transport in estuaries, p. 295–310. *In* J. Dronkers and W. van Leussen (eds.), Physical Processes in Estuaries. Springer-Verlag, Berlin.

Dyer, K. R., J. Cornelisse, M. P. Dearnaley, M. J. Fennessy, S. E. Jones, J. Kappenberg, I. N. McCave, M. Pejrup, W. Puls, W. van Leussen, and K. Wolfstein. 1996. A comparison of in situ techniques for estuarine floc settling velocity measurements. *Journal of Sea Research* 36:15–29.

Dyer, K. R. and E. M. Evans. 1989. Dynamics of turbidity maximum in a homogeneous tidal channel. *Journal of Coastal Research* SI:23–30.

Elliott, A. J., D. P. Wang, and D. W. Pritchard. 1978. The circulation near the head of Chesapeake Bay. *Journal of Marine Research* 36:643–655.

Festa, J. F. and D. V. Hansen. 1978. Turbidity maxima in partially mixed estuaries: A two-dimensional numerical model. *Estuarine and Coastal Marine Science* 7:347–359.

Geyer, W. R. 1993. The importance of suppression of turbulence by stratification on the estuarine turbidity maximum. *Estuaries* 16:113–125.

Geyer, W., R. Signell, and G. Kineke. 1998. Lateral trapping of sediment in a partially mixed estuary, p. 115–124. *In* J. Dronkers and M. Sheffers (eds.), Physics of Estuaries and Coastal Seas: Proceedings of the 8th International Biennial Conference on Physics of Estuaries and Coastal Seas. A. A. Balkema, Rotterdam, The Netherlands.

Grabemann, I., R. J. Uncles, G. Krause, and J. A. Stephens. 1997. Behaviour of turbidity maxima in the Tamar (UK) and Weser (FRG) estuaries. *Estuarine Coastal and Shelf Science* 45: 235–246.

Guezennec, L., R. Lafite, J. P. Dupont, R. Meyer, and D. Boust. 1999. Hydrodynamics of suspended particulate matter in the tidal freshwater zone of a macrotidal estuary (the Seine estuary, France). *Estuaries* 22:717–727.

Hamblin, P. F. 1989. Observations and model of sediment transport near the turbidity maximum of the upper Saint Lawrence estuary. *Journal of Geophysical Research* 94:14419–14428.

Hamblin, P. F., K. R. Lum, M. E. Comba, and K. L. E. Kaiser. 1988. Observations of suspended sediment flux over a tidal cycle in the region of the turbidity maximum of the upper St. Lawrence River Estuary, p. 245–256. *In* D. G. Aubrey and L. Weishar (eds.), Lecture Notes on Coastal and Estuarine Studies. Springer-Verlag, Berlin.

Hill, P. S. and T. G. Milligan. 1999. Suspicions about settling columns, p. 107–110. *In* Coastal Ocean Processes Symposium: A Tribute to William D. Grant. WHOI-99-04. Woods Hole Oceanographic Institute, Woods Hole, Massachusetts.

Hughes, M. G., P. T. Harris, and T. C. T. Hubble. 1998. Dynamics of the turbidity maximum zone in a micro-tidal estuary: Hawkesbury River, Australia. *Sedimentology* 45:397–410.

Jahmlich, S., L. Thomsen, and G. Graf. 1999. Factors controlling aggregate formation in the benthic boundary layer of the Mecklenburg Bight (western Baltic Sea). *Journal of Sea Research* 41:245–254.

Jay, D. A. and J. D. Musiak. 1994. Particle trapping in estuarine tidal flows. *Journal of Geophysical Research* 99:20445–20461.

Kerhin, R., J. P. Halka, D. V. Wells, E. L. Hennessee, P. J. Blakeslee, N. Zoltan, and R. H. Cuthbertson. 1988. The Surficial Sediments of Chesapeake Bay, Maryland: Physical Characteristics and Sediment Budget. Investigative Report No. 48. Maryland Geological Survey, Baltimore, Maryland.

Kimmerer, W. J., J. R. Burau, and W. A. Bennett. 1998. Tidally oriented vertical migration and position maintenance of zooplankton in a temperate estuary. *Limnology and Oceanography* 43:1697–1709.

Morgan, C. A., J. R. Cordell, and C. A. Simenstad. 1997. Sink or swim? Copepod population maintenance in the Columbia River estuarine turbidity-maxima region. *Marine Biology* 129: 309–317.

NICHOLS, M. 1974. Development of the turbidity maximum in the Rappahannock Estuary. *Memoires de l'Institute de Geologie du Bassin d'Aquitaine* 7:19–25.

NICHOLS, M. M. 1977. Response and recovery of an estuary following a river flood. *Journal of Sedimentary Petrology* 47:1171–1186.

NORTH, E. AND E. D. HOUDE. 2001. Retention of white perch and striped bass larvae: Biological-physical interactions in Chesapeake Bay estuarine turbidity maximum. *Estuaries* 24: 756–769.

OFFICER, C. B. 1980. Discussion of the turbidity maximum in partially mixed estuaries. *Estuarine and Coastal Marine Science* 10:239–246.

OFFICER, C. B., D. R. LYNCH, AND G. H. SETLOCK. 1984. Recent sedimentation rates in Chesapeake Bay, p. 131–157. *In* V. S. Kennedy (ed.), The Estuary as a Filter. Academic Press, Orlando, Florida.

OWEN, M. W. 1976. Determination of the Settling Velocities of Cohesive Muds. Hydraulics Research, Wallingford, United Kingdom.

PAK, H., D. A. KIEFER, AND J. C. KITCHEN. 1988. Meridional variations in the concentration of chlorophyll and microparticles in the North Pacific Ocean. *Deep Sea Research* 35:1151–1171.

PANAGEOTOU, W., C. WILLIAMS, R. ORTT, AND J. HALKA. 1998. Placement, consolidation and erosion studies of sediments dredged from the approach channel to the Chesapeake and Delaware Canal, November, 1996–February, 1997. Maryland Geological Survey, Baltimore, Maryland.

ROMAN, M. R., D. V. HOLLIDAY, E. D. HOUDE, AND L. P. SANFORD. 1997. Temporal and spatial patterns of zooplankton in the Chesapeake Bay turbidity maximum. CM. 1997/S:18. International Council for the Exploration of the Sea, Copenhagen, Denmark.

ROMAN, M. R., D. V. HOLLIDAY, AND L. P. SANFORD. 2001. Temporal and spatial patterns of zooplankton in the Chesapeake Bay turbidity maximum. *Marine Ecology Progress Series* 213:215–227.

SANFORD, L. P. 1994. Wave forced erosion of bottom sediments in upper Chesapeake Bay. *Estuaries* 17:148–165.

SANFORD, L. P. AND M.-L. CHANG. 1997. The bottom boundary condition for suspended sediment deposition. *Journal of Coastal Research* 25:3–17.

SANFORD, L. P. AND J. P. HALKA. 1993. Assessing the paradigm of mutually exclusive erosion and deposition of mud, with examples from upper Chesapeake Bay. *Marine Geology* 114:37–57.

SANFORD, L. P., W. PANAGEOTOU, AND J. P. HALKA. 1991. Tidal resuspension of sediments in northern Chesapeake Bay. *Marine Geology* 97:87–103.

SCHUBEL, J. R. 1968a. Suspended Sediment of the Northern Chesapeake Bay. The Chesapeake Bay Institute of the Johns Hopkins University, Baltimore, Maryland.

SCHUBEL, J. R. 1968b. Turbidity maximum of the northern Chesapeake Bay. *Science* 161:1013–1015.

SCHUBEL, J. R. 1971. Tidal variation of the size distribution of suspended sediment at a station in the Chesapeake Bay turbidity maximum. *Netherlands Journal of Sea Research* 5:252–266.

SCHUBEL, J. R. AND R. B. BIGGS. 1969. Distribution of seston in upper Chesapeake Bay. *Chesapeake Science* 10:18–23.

SCHUBEL, J. R. AND T. W. KANA. 1972. Agglomeration of fine-grained suspended sediment in northern Chesapeake Bay. *Powder Technology* 6:9–16.

SCHUBEL, J. AND D. PRITCHARD. 1986. Responses of upper Chesapeake Bay to variations in discharge of the Susquehanna River. *Estuaries* 9:236–249.

SETZLER-HAMILTON, E. M. 1991. White perch, p. 12-1-12-20. *In* S. L. Funderburk, J. A. Mihursky, S. J. Jordan, and D. Riley (eds.), Habitat Requirements for Chesapeake Bay Living Resources, 2nd Edition. Living Resources Subcommittee, Chesapeake Bay Program, Maryland Department of Natural Resources, Annapolis, Maryland.

SETZLER-HAMILTON, E. M. AND L. HALL, JR. 1991. Striped bass, p. 13-1-13-31. *In* S. L. Funderburk, J. A. Mihursky, S. J. Jordan, and D. Riley (eds.), Habitat Requirements for Chesapeake Bay Living Resources, 2nd Edition. Living Resources Subcommittee, Chesapeake Bay Program, Maryland Department of Natural Resources, Annapolis, Maryland.

SIMENSTAD, C. A., C. A. MORGAN, J. R. CORDELL, AND J. A. BAROSS. 1994. Flux, passive retention, and active residence of zooplankton in Columbia River estuarine turbidity maxima, p. 473–482. *In* K. R. Dyer, and R. J. Orth (eds.), Changes in Fluxes in Estuaries: Implications from Science to Management. Olsen and Olsen, Fredensborg, Denmark.

UNCLES, R. J., A. E. EASTON, M. L. GRIFFITHS, C. HARRIS, R. J. M. HOWLAND, R. S. KING, A. W. MORRIS, AND D. H. PLUMMER. 1998. Seasonality of the turbidity maximum in the Humber-Ouse estuary, UK. *Marine Pollution Bulletin* 37:206–215.

UNCLES, R. J. AND J. A. STEPHENS. 1993. The freshwater-saltwater interface and its relationship to the turbidity maximum in the Tamar Estuary, United Kingdom. *Estuaries* 16:126–141.

YOCHUM, S. E. 2000. A revised load estimation procedure for the Susquehanna, Potomac, Patuxent, and Choptank Rivers. Water-Resources Investigations Report 00–4156. U.S. Geological Survey, Baltimore, Maryland.

ZIMMERMANN-TIMM, H., H. HOLST, AND S. MULLER. 1998. Seasonal dynamics of aggregates and their typical biocoenosis in the Elbe Estuary. *Estuaries* 21:613–621.

ZYNJUK, L. AND B. MAJEDI. 1996. January 1996 Floods Deliver Large Loads of Nutrients and Sediment to the Chesapeake Bay. Fact Sheet FS-140–96. U.S. Geological Survey, Reston, Virginia.

Received for consideration, May 26, 2000
Accepted for publication, March 8, 2001